A juxta-membrane amino acid sequence of P-selectin glycoprotein ligand-1 is involved in moesin binding and ezrin/radixin/moesin-directed targeting at the trailing edge of migrating...

ARTICLE *in* EUROPEAN JOURNAL OF IMMUNOLOGY · JULY 2002

Impact Factor: 4.03 · DOI: 10.1002/1521-4141(200206)32:6<1560::AID-IMMU1560>3.0.CO;2-U · Source: PubMed

8 AUTHORS, INCLUDING:

Juan M Serrador
Spanish National Research Council
28 PUBLICATIONS **2,234** CITATIONS
SEE PROFILE

Ana Urzainqui
Hospital Universitario de La Princesa
35 PUBLICATIONS **1,377** CITATIONS
SEE PROFILE

Maria Montoya
Spanish National Centre for Cardiovascular …
35 PUBLICATIONS **2,281** CITATIONS
SEE PROFILE

María Yáñez-Mó
Hospital Universitario de La Princesa
77 PUBLICATIONS **4,190** CITATIONS
SEE PROFILE

A juxta-membrane amino acid sequence of P-selectin glycoprotein ligand-1 is involved in moesin binding and ezrin/radixin/moesin-directed targeting at the trailing edge of migrating lymphocytes

Juan M. Serrador, Ana Urzainqui, Jose L. Alonso-Lebrero, J. Román Cabrero, Maria C. Montoya, Miguel Vicente-Manzanares, María Yáñez-Mó and Francisco Sánchez-Madrid

Servicio de Inmunología, Hospital de la Princesa, Universidad Autónoma de Madrid, Madrid, Spain

P-selectin glycoprotein ligand 1 (PSGL-1) is an adhesion receptor localized on the tips of microvilli that is involved in the rolling of neutrophils on activated endothelium. We found that PSGL-1 was concentrated at the uropod of chemokine-stimulated lymphoid cells. Dynamic fluorescence videomicroscopy analyses of migrating lymphocytes demonstrated that PSGL-1 and moesin redistributed towards the cellular uropod at the trailing edge of these cells, where activated ezrin/radixin/moesin (ERM) proteins were located. An eighteen amino acid sequence in the juxta-membrane region of the PSGL-1 cytoplasmic tail was found to be critical for uropod targeting and moesin binding. Substitution of S336, S348, and the basic cluster R337K338 by alanines within this region significantly impaired both moesin binding and PSGL-1 polarization. These results underline the role of moesin in the subcellular redistribution of PSGL-1 in lymphoid cells and make evident the importance of specific serine residues within the cytoplasmic tail of PSGL-1 for this process.

Received	16/12/02
Revised	25/2/02
Accepted	8/3/02

Key words: Lymphocyte / Uropod / Cytoskeleton / Cell migration / Polarization

1 Introduction

Selectins have a key role in the migration of leukocytes into inflammatory foci, mainly mediating the initial tethering and rolling of leukocytes on the activated endothelium [1]. P- and E-selectins, expressed by activated endothelial cells, and L-selectin on leukocytes bind to P-selectin glycoprotein ligand-1 (PSGL-1), a mucin-like adhesion receptor of 120 kDa detected on most leukocytes [2]. PSGL-1 is clustered on the tips of leukocyte microvilli, facilitating the initial contact with endothelium during transendothelial migration [3].

Earlier studies showed that cellular uropods are enriched in microvilli and microspikes [4]. PSGL-1 is concentrated on the uropods of neutrophils activated with platelet-activating factor [5], where it co-localizes with ezrin and moesin [6]. Ezrin, radixin and moesin (ERM proteins) are also localized on the tips of leukocyte microvilli [7]. These proteins have two conserved domains, the amino-terminal domain is responsible for plasma membrane localization, whereas the C-terminal domain has a consensus F-actin binding motif. Through these domains ERM proteins connect adhesion receptors with cytoskeleton, and they regulate the protrusive activity required for microvilli formation [8, 9–11]. Since the molecules responsible of the redistribution of PSGL-1 have not been characterized, we decided to investigate the dynamics of the interaction of ERM proteins with PSGL-1 and to look for the specific residues in the cytoplasmic domain of this adhesion receptor involved in moesin binding and uropod targeting.

[I 22715]

Abbreviations: GFP: Green fluorescent protein **GST:** Glutathione-S-transferase **N-ezrin:** N-terminal domain of ezrin **N-moesin:** N-terminal domain of moesin **PSGL-1:** P-selectin glycoprotein ligand-1 **ERM:** Ezrin/radixin/moesin **TIL:** Tumor-infiltrating lymphocytes

2 Results

The expression, function and subcellular localization of PSGL-1 have been characterized in myeloid cells [2, 12]. However, less is known about the role of PSGL-1 in cells

0014-2980/02/0606-1560$17.50+.50/0

of the lymphoid lineage. We therefore decided to analyze the subcellular localization of PSGL-1 in lymphoid cells. We found that PSGL-1 was concentrated in the uropod of PBL and T lymphoblasts stimulated with the chemokine RANTES (Fig. 1A). In contrast, no redistribution of PSGL-1 was observed in the plasma membrane of non-polarized peripheral blood lymphocytes (PBL) and T lymphoblasts (data not shown). PSGL-1 was also concentrated in the uropods of TIL and NK cells stimulated with IL-2 as well as in the constitutively polarized lymphoblastoid cell lines HSB-2 and Peer (Fig. 1A).

It has been described that moesin and ezrin, the two ERM proteins which are highly expressed in leukocytes, co-localize with PSGL-1 in the uropods of neutrophils [6]. In order to gain insight into the mechanisms responsible for the concentration of PSGL-1 in the uropods of migrating lymphocytes, we generated PSGL-1-GFP and moesin-GFP fusion proteins. These proteins were expressed in migrating NS1 cells, a constitutively polarized mouse myeloma cell line, and their dynamic redistribution was monitored by time-lapse fluorescence confocal microscopy. PSGL-1-GFP and moesin-GFP accumulated at the rear of migrating cells (Fig. 1B and C, respectively). In these cells, PSGL-1-GFP tended to be clustered at the cellular uropod (Fig. 1B), whereas moesin-GFP was restricted to this subcellular domain (Fig. 1C). The activation of ERM proteins by phosphorylation of a conserved threonine in the C-terminal domain regulates the morphogenesis of membrane projections [13, 14]. To examine the distribution of activated ERM proteins, NS1 cells were stained with the rat 297S mAb, which recognizes C-terminal phosphorylated ERM proteins [15]. We found that phosphorylated ERM proteins were concentrated in the uropod of migrating cells (Fig. 1D). Although this finding strongly suggests that activated ERM proteins are involved in the redistribution of PSGL-1 towards the uropod of migrating lymphocytes, the involvement of other linker proteins can not be excluded.

To identify the cytoplasmic region of PSGL-1 that is responsible for its localization at the cellular uropod, the distribution of C-terminal deletion mutants of PSGL-1 expressed in NS1 cells was studied (Fig. 2A). All truncated proteins as well as the wild-type PSGL-1 were mainly concentrated at the uropod. However, the tailless S336stop protein was uniformly distributed throughout the plasma membrane (Fig. 2B). Interestingly, E385stop and P366stop proteins had a membrane distribution similar to the wild-type protein, whereas M352stop and R345stop proteins were restricted to the uropod

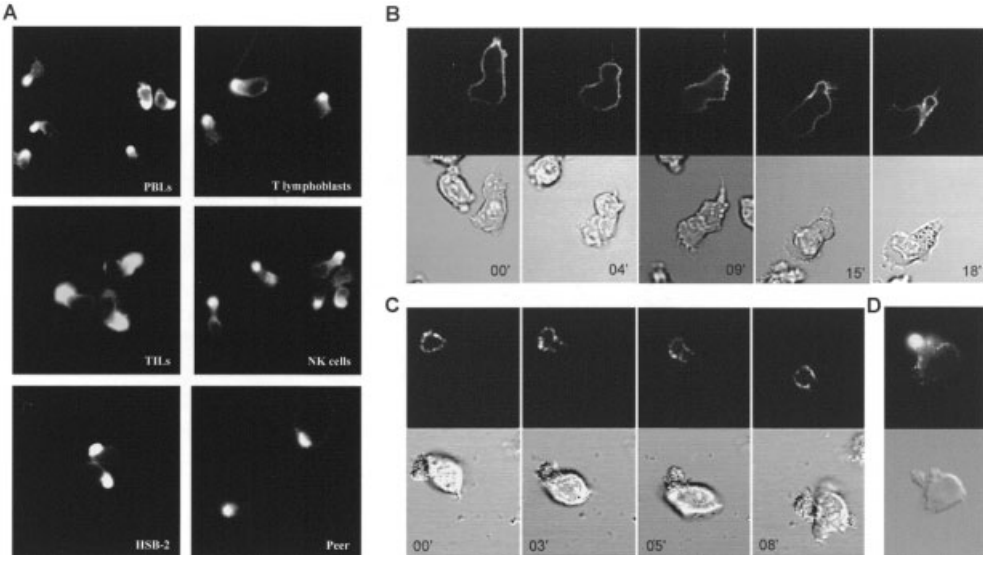

Fig. 1. Dynamic localization of moesin and PSGL-1 in migrating lymphoid cells. (A) Immunofluorescence analysis of PSGL-1 in cells of lymphoid lineage. RANTES-stimulated PBL, T lymphoblasts, NK cells, TIL, and HSB-2 and Peer lymphoblastoid cells were allowed to adhere to FN-80-coated glass coverslips for 20 min. Then, cells were fixed and stained for PSGL-1 using the PL-1 mAb. (B, C, and D) Dynamics of moesin and PSGL-1 redistribution during lymphocyte migration. NS1 cells were transiently transfected with moesin-GFP or PSGL-1-GFP and live imaging was performed by three-dimensional fluorescence microscopy. Series of images showing fluorescence of PSGL-1-GFP (B) and moesin-GFP (C) of migrating NS1 cells were obtained at the indicated times. In (D), activated ERM proteins were detected using the rat 297S mAb. The corresponding DIC images are shown below.

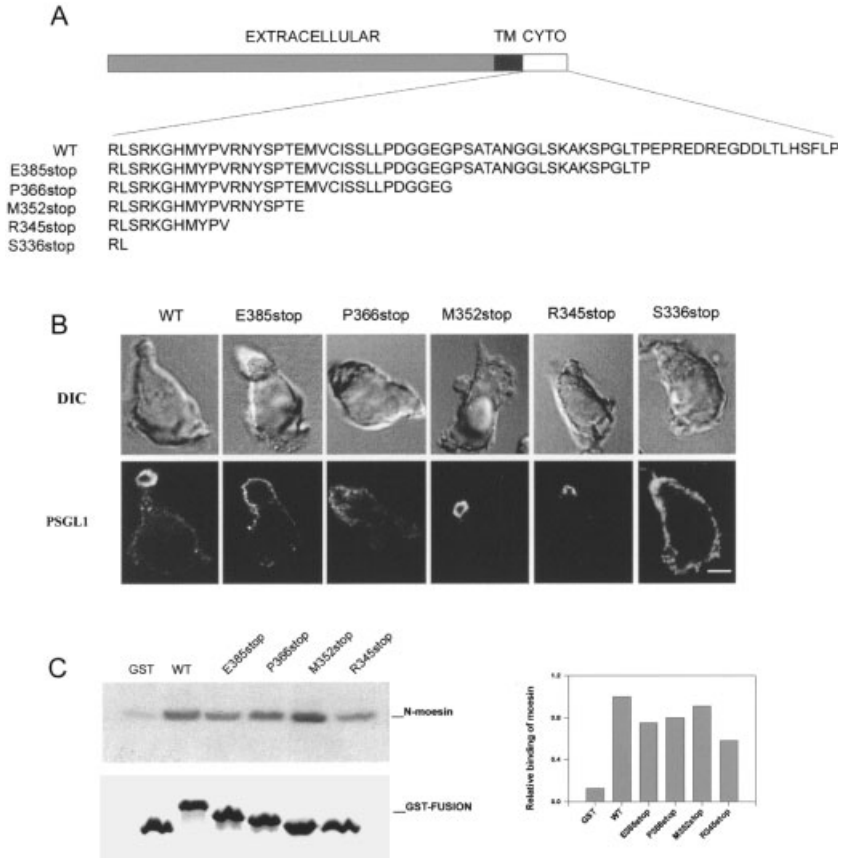

Fig. 2. Involvement of the juxta-membrane region of PSGL-1 cytoplasmic tail in ERM binding and uropod targeting. (A) Schematic representation of wild-type (WT) PSGL-1, and deletions in the cytoplasmic domain of PSGL-1. Residues were numbered according the amino acid sequence of PSGL-1 as described by Sako et al. [12]. (B) Subcellular localization by immunofluorescence microscopy of WT and PSGL-1 truncated proteins. WT and C-terminal truncations of PSGL-1 were transiently expressed in NS1 cells, and stained with the anti-PSGL-1, PL-2 mAb. Corresponding DIC pictures are shown on top. Bar, 4 μm. (C) Association of PSGL-1 truncated proteins with N-moesin. GST or GST fusion proteins of WT and truncated forms of PSGL-1 were bound to glutathione Sepharose beads and then incubated with [^{35}S]methionine-labeled N-moesin. Proteins were eluted by boiling samples. Coomassie staining of GST fusion proteins is also shown. Relative binding of N-moesin to GST fusion proteins was estimated by densitometric analysis comparing the amount of moesin bound to equal amounts of each mutant with that eluted from PSGL-1WT, as described previously by Yonemura et al. [9].

(Fig. 2B). All truncated proteins polarized to the cellular uropod to a similar extent as wild-type PSGL-1 with the exception of S336stop and R345stop mutations (Table 1). Endogenous PSGL-1 was not detected in NS1 cells (data not shown).

To determine the relationship between PSGL-1-ERM binding and uropod localization, GST fusion proteins of different PSGL-1 deletion mutations were generated and analyzed for their binding to isotope-labeled N-moesin and N-ezrin, the N-terminal domains of ERM proteins that bind PSGL-1 [6]. E385stop, P366stop and M352stop bound N-moesin at similar extent than wild-type PSGL-1, whereas the binding of N-moesin to R345stop was somewhat lower (Fig. 2C). Similar results were obtained with N-ezrin (data not shown). These data indicate that the residues involved in moesin binding and receptor polarization are located within the first 18 amino acids of the juxta-membrane region of PSGL-1.

Clusters of positively charged amino acids in transmembrane proteins have been implicated in the binding to ERM proteins [9]. Therefore, we decided to carry out a mutational analysis of the positively charged cluster R337-K338 within this 18-amino acid region. In addition to these two residues, S336, H340, Y342, and S348 were replaced by A and their binding to N-moesin was examined (Fig. 3A). Mutant proteins R337K338→AA, S336A and S348A bound to a lesser extent to N-moesin than wild type PSGL-1, or the Y342A mutant protein (Fig. 3B).

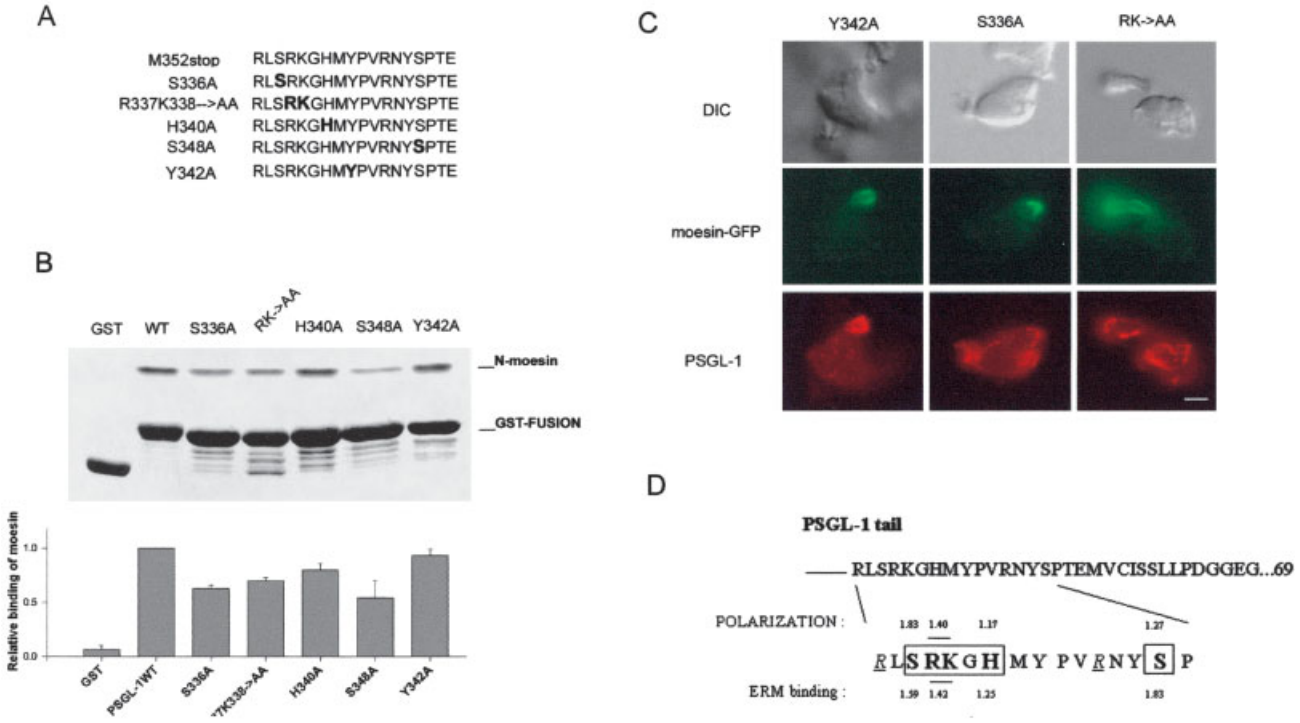

Fig. 3. Amino acid residues of the juxta-membrane cytoplasmic tail of PSGL-1 involved in their subcellular targeting and ERM binding. (A) Schematic representation of M352stop truncation, double and point mutations in the cytoplasmic domain of PSGL-1. (B) Association of mutated PSGL-1 with N-moesin. Binding of [S^{35}]-labeled N-moesin to the GST-cytoplasmic point mutations of PSGL-1 was carried out as in (Fig. 2C). Values correspond to the arithmetic mean ± SD of the relative binding capability from three independent experiments. (C) NS1 cells were transiently co-transfected with full-length moesin-GFP (green) and the mutated forms of PSGL-1 (red). Cells were stained with the anti-PSGL-1 PL-2 mAb. Bar, 6 μm. (D) The residues of PSGL-1 important for its polarization and ERM binding are represented in bold letters. Motifs important for PSGL-1 targeting and ERM binding are remarked within boxes, and arginines near these motifs are underlined. The contribution of each analyzed residue to ERM binding and PSGL-1 polarization is represented by an index. Polarization values were calculated as the inverse of the ratio of polarization between the percent of cells expressing each mutant and the 18 amino acid-containing M352stop mutant (Table 1). Corresponding values of ERM binding were calculated as the inverse of the relative mean binding of moesin and ezrin (B, and data not shown).

In addition, H340A mutation also rendered weaker moesin binding compared to the wild-type protein (Fig. 3B). Similar results were obtained with N-ezrin (data not shown). When these PSGL-1 mutant proteins were expressed in NS1 cells, S336A, R337K338→AA, and S348A showed a decreased concentration at the uropod, whereas the polarization of H340A only exhibited a mild diminution. The distribution of Y342A was similar to that of wild-type protein (Table 1). Co-expression studies of these mutated proteins and full-length moesin-GFP in NS1 cells showed a strong co-localization in the uropod of Y342A and moesin-GFP (Fig. 3C), whereas S336A and R337K338→AA mutants were evenly distributed through the plasma membrane, in clear contrast with the strong concentration of GFP-moesin in the uropod (Fig. 3C). Hence, the positively charged residues R337K338 and a motif comprising S336 and to a lower extent S348 are important for the ERM-directed redistribution of PSGL-1 towards the uropod of migrating lymphocytes (Fig 3D).

3 Discussion

It has been demonstrated that PSGL-1 plays an important role in the tethering and rolling of polymorphonuclear neutrophils on endothelium through its binding to P- and E-selectins [3, 16]. However, this function is not restricted to neutrophils, and PSGL-1 mediates the selective recruitment of Th1 lymphocytes into delayed-type hypersensitivity reactions of the skin [17, 18]. Prior to their rolling step, leukocytes must establish contact with endothelial cells. Leukocyte tethering is mediated by adhesion receptors located at the tips of microvilli,

Table 1. Quantitative analysis of the redistribution to the uropod of PSGL-1 mutant proteins

Mutant	Cell number (counts)	PSGL-1-redistributed	% Polarization[a)]
PSGL-1 WT	449	349	77.7
S336stop	220	65	29.5
R345stop	321	195	60.7
M352stop	200	150	75.0
P366stop	450	370	82.2
E385stop	356	283	79.4
S336A	301	123	40.9
R337K338→AA	294	157	53.4
H340A	312	200	64.1
Y342A	334	245	73.3
S348A	280	165	58.9

a) Percent of polarization corresponds to the total number of PSGL-1-redistributed cells to the uropod divided by the total number of transfected, morphologically polarized cells. Total counts of four independent experiments are shown.

and PSGL-1 is the major selectin ligand on these membrane projections [19]. In this regard, ERM proteins in conjunction with adhesion receptors are responsible for the cell cortex organization of microvilli [8, 14]. The ERM-directed redistribution of PSGL-1 could facilitate the initial cell tethering by clustering of this receptor. Accordingly, it has been shown that PSGL-1 dimerization stabilizes tethering and rolling by rebinding to their ligands [20]. However, the redistribution of PSGL-1 towards the cellular uropod of activated neutrophils disengages it from P-selectin and facilitates transendothelial migration [5]. Data showing an activated status of PSGL-1 during its redistribution has not been reported so far, in spite of the fact that the activation of lymphocytes increases the binding of PSGL-1 to P-selectin [21]. It is feasible that ERM-directed redistribution of PSGL-1 towards the cellular uropod may represent a mechanism of ligand dissociation through the modification of the local topography of this receptor without changes in ligand affinity. In this regard, P-selectin binds to the uropod of polarized neutrophils and lymphocytes ([5] and Serrador et al., unpublished data), suggesting that active PSGL-1 molecules are localized in this subcellular area. These data further support the issue that adhesion receptors in the uropods of leukocytes facilitate the recruitment of other leukocytes leading to secondary tethering and amplifying transendothelial migration [2, 22, 23]. On the other hand, our results make evident the key role of moesin in the localization of mucin-like molecules at defined membrane domains. In this regard, it has been recently described that moesin is responsible for the exclusion of CD43 from the T cell-APC contact zone [24]. We have also found that PSGL-1 is excluded from the immunological synapse [25]. In summary, our data provide evidence that PSGL-1 redistribution on the plasma membrane of lymphocytes is directed by ERM proteins, and that this phenomenon is selectively regulated by serines near a positively charged cluster within its juxtamembrane region.

4 Materials and methods

4.1 Antibodies, cells and reagents

The anti-PSGL-1 PL-1 and PL-2 mAb were kindly provided by Dr. R. McEver (W. K. Warren Medical Research Institute, Oklahoma, OK). The rat 297S mAb specific for mouse phosphorylated threonine at the C terminus of each ERM was generously provided by Dr. S. Tsukita (Department of Cell Biology, Kyoto University, Japan). P3X63 myeloma protein (IgG1, kappa) was used as negative control. PBL were isolated from fresh human blood by density gradient centrifugation, followed by adherence on plastic flasks. Human T lymphoblasts were prepared from 48 h phytohemagglutinin-treated blood mononuclear cells. TIL were isolated from patients with metastatic melanoma (Department of Pathology, Hospital General Gregorio Marañón, Madrid, Spain). To obtain IL-2-activated NK cells, PBL were cultured with irradiated (5 Gy) RPMI 8866 lymphoblastoid cells for 6 to 9 days in RPMI supplemented with 10% FCS, followed by a negative selection step using an anti-CD3 mAb plus rabbit complement (Behring, Marburg, Germany). The HSB-2 and Peer human T cell lines, and the mouse myeloma NS1 cell line were grown in RPMI 1640 culture medium (Gibco BRL, Gaithersburg, MD) supplemented with 10% FCS. Recombinant human RANTES was obtained from R&D Systems (Minneapolis, MN).

4.2 Recombinant DNA constructs and transfection of cells

For PSGL-1 cell expression, the pCDNA3 plasmid carrying full-length PSGL-1 wild type was used. PSGL-1 deletion mutations were obtained by PCR using PSGL-1 cDNA as template, PSGL-N [GGGCCCGGATCCAGATCTATGC CTCTGCAACTCCTCCTG] as 5' primer and the following 3' primers: S336stop [GAGGCGGACCGCCAGCACCAC]; R345stop [CACGGGGTACATGTGGCCCTT]; M352stop [CTCGGTGGGGGAGTAATTACG]; P366stop [CCCCTCACCCCCATCAGGCAA]; and E385stop [TGGCGTCAGGCCCGG GCTCTT]. All the 3' primers have two stop codons, and a PstI restric-

tion site to facilitate posterior subcloning. To generate point and double mutations of PSGL-1, the following replacements of codons were performed: CGCAAG to GCCGCG (R337K338→AA); TCC to GCC (S336A); CAC to GCC (H340A); TCC to GCC (S348A). All mutations were verified by nucleotide sequencing.

Human PSGL-1 cDNA lacking the stop codon was subcloned into pEGFP-N1 (Clontech, Palo Alto, CA) by using EcoRI and HindIII, and resulting in an in-frame fusion of GFP to the C terminus of PSGL-1. The generation of the GFP fusion construct with the GFP cDNA inserted at the C-terminal end of full-length (residues 1–577) rat moesin was described previously [26]. Transiently transfected NS1 cells were generated by electroporation basically as previously described [26]. After electroporation burst, NS1 cells were transferred to coverslips in flat-bottom 24-well plates (Costar, Cambridge, MA) in a final volume of 1 ml complete medium + 50 μM β-mercaptoethanol (Sigma). After 24 h of transfection, cells were fixed in 3.7% formaldehyde in PBS for 10 min at room temperature and rinsed in TBS (50 mM Tris-HCl, 150 mM NaCl, pH 7.6).

4.3 Immunofluorescence microscopy and time-lapse fluorescence videomicroscopy

Transiently transfected NS1 cells were visualized by staining the cells with the anti-PSGL-1 PL-2 mAb plus a 1:50 dilution of an FITC-labeled goat $F(ab')_2$ anti-mouse Ig (Dako). Cells were observed using a Leica DMR photomicroscope (Leica, Mannheim, Germany) with 40, 63, and 100× oil immersion objectives. Images were acquired using the Leica QFISH 1.0 software. The proportion of PSGL-1-redistributed cells was calculated by random choice of ten different fields (60× objective) of each condition and counting of at least 200 cells. To carry out time-lapse fluorescence videomicroscopy, coverslips were mounted on Attofluor open chambers (Molecular Probes, Eugene, OR) and placed on the microscope stage. Cells were maintained at 37°C in a 5% CO_2 atmosphere using an incubation system [La-con (GBr) Pecon (GmbH)]. Confocal images were acquired using a Leica TCS-SP confocal laser-scanning unit equipped with Ar and He/Ne laser beams and attached to a Leica DMIRBE inverted epifluorescence microscope. Series of fluorescence and differential interference contrast (DIC) images were obtained simultaneously at 1-min intervals starting 36 h after the initiation of the plasmid electroporation of NS1 cells. Optical sectioning of cells was necessary to capture all of the fluorescence signal. A section of the middle fluorescence images is presented with its corresponding DIC image.

4.4 Construction, expression and purification of GST fusion proteins, *in vitro* translation and binding assays

Construction of the GST fusion protein with the cytoplasmic regions of human PSGL-1 has been reported elsewhere [6]. Constructs coding for deletion and point mutation cytoplasmic variants of both proteins were performed by oligonucleotide site-directed mutagenesis either by overlap extension or site-directed mutagenesis. The pCR3 plasmids carrying the inserts of untagged moesin and ezrin amino-terminal regions containing amino acid residues 1–310 (MSNn/pCR3 and EZR/pCR3, respectively) were described previously [27]. Plasmids were transcribed and translated *in vitro* using a TNT-coupled rabbit reticulocyte lysate system (Promega, Madison, WI) in the presence of T7 RNA polymerase and L-[^{35}S]methionine. Protein-protein binding assays were carried out as previously described [6].

Acknowledgement: We thank Dr. H. Furthmayr, for kindly providing moesin and ezrin constructs and for critical reading of the manuscript, Dr. R. Gonzalez-Amaro for critical readings of the manuscript and L. Huang and P. Litman for preparing constructs for expression and *in vitro* translation studies. This work was supported by grants SAF99–0034-C01 and FEDER 2FD97–068-C02–02 from Ministerio de Educación, grant 08.3/0010.1/99 from Comunidad Autónoma de Madrid, and grant from European Community QLRT-1999–01036.

References

1 **Springer, T. A.,** Traffic signals for lymphocyte recirculation and leukocyte emigration: The multistep paradigm. *Cell* 1994. **76:** 301–314.

2 **McEver, R. and Cummings, R.,** Role of PSGL-1 binding to selectins in leukocyte recruitment. *J. Clin. Invest*. 1997. **100:** 485–491.

3 **Moore, K., Patel, K., Bruehl, R., Fugang, L., Johnson, D., Lichenstein, H., Cummings, R., Bainton, D. and McEver, R.,** P-selectin glycoprotein ligand-1 mediates rolling of human neutrophils on P-selectin. *J. Cell Biol*. 1995. **128:**661–671.

4 **McFarland, W.,** Microspikes on the lymphocyte uropod. *Science* 1969. **163:** 818–820.

5 **Lorant, D., McEver, R., McIntrye, T., Moore, K., Prescott, S. and Zimmerman, G.,** Activation of polymorphonuclear leukocytes reduces their adhesion to P-selectin and causes redistribution of ligands for P-selectin on their surfaces. *J. Clin. Invest*. 1995. **96:** 171–182.

6 **Alonso-Lebrero, J. L, Serrador, J. M., Domínguez-Jiménez, C., Barreiro, O., Luque, A., del Pozo, M. A., Snapp, K., Kansas, G., Schwartz-Albiez, R., Furthmayr, H., Lozano, F. and Sánchez-Madrid, F.,** Polarization and interaction of adhesion molecules P-selectin glycoprotein ligand 1 and intercellular adhesion molecule 3 with moesin and ezrin in myeloid cells. *Blood* 2000. **95:** 2413–2419.

7 **Amieva, M. R. and Furthmayr, H.,** Subcellular localization of moesin in dynamic filopodia, retraction fibers, and other struc-

tures involved in substrate exploration, attachment, and cell-cell contacts. *Exp. Cell Res*. 1995. **219:** 180–196.

8 **Yonemura, S., Tsukita, Sa. and Tsukita, Sh.,** Direct involvement of ezrin/radixin/moesin (ERM)-binding membrane proteins in the organization of microvilli in collaboration with activated ERM proteins. *J. Cell Biol*. 1999. **145:** 1497–1509.

9 **Yonemura, S., Hirao, M., Doi, Y., Takahashi, N., Kondo, T., Tsukita, Sa. and Tsukita, Sh.,** Ezrin/radixin/moesin (ERM) protein bind to a positively charged amino acid cluster in the juxtamembrane cytoplasmic domain of CD44, CD43, and ICAM-2. *J. Cell Biol*. 1998. **140:** 885–895.

10 **Heiska, L., Alfthan, K., Grönholm, M., Vilja, P., Vaheri, A. and Carpen, O.,** Association of ezrin with intercellular adhesion molecule-1 and -2 (ICAM-1 and ICAM-2). *J. Biol. Chem*. 1998. **273:** 21893–21900.

11 **Ivetic, A., Deka, J., Ridley, A. and Ager, A.,** The cytoplasmic tail of L-selectin interacts with members of the ezrin-radixin-moesin (ERM) family of proteins: Activation dependent binding of moesin but not ezrin. *J. Biol. Chem*. 2001. **277:** 2321–2329.

12 **Sako, D., Chang, X. J., Barone, K. M., Vachino, G., White, H. M., Shaw, G., Veldman, G. M., Bean, K. M., Ahern, T. J. and Furie, B.,** Expression cloning of a functional glycoprotein ligand for P-selectin. *Cell* 1993.**75:** 1179–1186.

13 **Matsui, T., Maeda, M., Doi, Y., Yonemura, S., Amano, M., Kaibuchi, K. and Tsukita, S.,** Rho-kinase phosphorylates COOH-terminal threonines of ezrin/radixin/moesin (ERM) proteins and regulates their head-to-tail association. *J. Cell Biol*. 1998. **140:**647–657.

14 **Gautreau, A., Louvard, D. and Arpin, M.,** Morphogenic effects of ezrin require a phosphorylation-induced transition from oligomers to monomers at the plasma membrane. *J. Cell Biol*. 2000. **150:**193–203.

15 **Hayashi, K., Yonemura, S., Matsui, T., Tsukita, Sa. and Tsukita, Sh.,** Immunofluorescence detection of ezrin/radixin/moesin (ERM) proteins with their carboxyl-terminal threonine phosphorylated in cultured cells and tissues. *J. Cell. Sci*. 1999. **112:** 1149–1158.

16 **Yang, J., Hirata, T., Croce, Merrill-Skoloff, K., Tchernychev, B., Williams, E., Flaumenhaft, R., Furie, B. C. and Furie, B.,** Targeted gene disruption demonstrates that P-selectin glycoprotein ligand 1 (PSGL-1) is required for P-selectin-mediated but not E-selectin-mediated neutrophil rolling and migration. *J. Exp. Med*. 1999. **20:** 1769–1782.

17 **Borges, E., Tietz, W., Steegmaier, M., Moll, T., Hallmann, R., Hamann, A. and Vestweber, D.,** P-selectin glycoprotein ligand-1 (PSGL-1) on T helper 1 but not on T helper 2 cells bind to P-selectin and supports migration into inflamed skin. *J. Exp. Med*. 1997. **185:** 573–578.

18 **Hirata, T., Merrill-Skoloff, G., Aab, M., Yang, J., Furie, B. C. and Furie, B.,** P-selectin glycoprotein ligand 1 (PSGL-1) is a physiological ligand for E-selectin in mediating T helper 1 lymphocyte migration. *J. Exp. Med*. 2000. **192:** 1669–1675.

19 **Smidtke, D. and Diamond, S.,** Direct observation of membrane tethers formed during neutrophil attachment to platelets or P-selectin under physiological flow. *J. Cell Biol*. 2000. **149:**719–729.

20 **Ramachandran, V., Yago, T., Epperson, T., Kobzdej, M., Nollert, M., Cummings, R., Zhu, C. and McEver, R.,** Dimerization of a selectin ligand stabilizes cell rolling and enhances tether strength in shear flow. *Proc. Natl. Acad. Sci. USA* 2001. **98:** 10166–10171.

21 **Vachino, G., Chang, X., Veldman, G., Kumar, R., Sako, D., Fouser, L., Berndt, M. and Cummings, D.,** P-selectin glycoprotein ligand-1is the major counter-receptor for P-selectin on stimulated T cells and is widely distributed in non-functional form on many lymphocytic cells. *J. Biol. Chem*. 1995. **270:** 21966–21974.

22 **Del Pozo, M. A., Cabañas, C., Montoya, M., Ager, A., Sánchez-Mateos, P. and Sánchez-Madrid, F.,** ICAMs redistributed by chemokines to cellular uropods as a mechanism for recruitment of T lymphocytes. *J. Cell Biol*. 1997. **137:** 493–508.

23 **Alon, R., Fuhlbrigge, R., Finger, E. and Springer, T. A.,** Interactions through L-selectin between leukocytes and adherent leukocytes nucleate rolling adhesions on selectins and VCAM-1 in shear flow. *J. Cell Biol*. 1996. **135:** 849–865.

24 **Allenspach, E. J., Cullinan, P., Tong, J., Tang, Q., Tesciuba, A.G., Cannon, J. L., Takahashi, S. M., Burkhardt, J. K. and Sperling, A. I.,** ERM-dependent movement of CD43 defines a novel Protein complex distal to the immunological synapse. *Immunity* 2001. **15:** 739–750.

25 **Montoya, M. C., Sancho, D., Bonello, G., Collette, Y., Langlet, C., He, H. T., Aparicio, P., Alcover, A., Olive, D. and Sánchez-Madrid, F.,** Role of ICAM-3 in the initial interaction of T lymphocytes and antigen presenting cells. *Nature Immunol*. 2002. **3:** 159–168.

26 **Amieva, M. R., Litman, P., Huang, L., Ichimaru, E. and Furthmayr, H.,** Disruption of dynamic cell surface architecture of NIH3T3 fibroblasts by the N-terminal domains of moesin and ezrin: *in vivo* imaging with GFP fusion proteins. *J. Cell Sci*. 1999. **112:** 111–125.

27 **Huang, L., Won, T., Lin, R. and Furthmayr, H.,** Replacement of 558 threonine, a critical site of phosphorylation of moesin *in vivo*, with aspartate activates F-actin binding of moesin: regulation by conformational change. *J. Biol. Chem*. 1999. **274:** 12803–12810.

Correspondence: Francisco Sánchez-Madrid, Servicio de Inmunología, Hospital de la Princesa, Universidad Autónoma de Madrid, Madrid, Spain
Fax: +34-91-520-2374
e-mail: fsanchez@hlpr.insalud.es